Available online at www.sciencedirect.com

ScienceDirect

Procedia Engineering 116 (2015) 390 – 397

Procedia Engineering

www.elsevier.com/locate/procedia

8th International Conference on Asian and Pacific Coasts (APAC 2015)

Edge waves generated by external forces

Seung-Nam Seo[a,b,*]

[a]*Coastal & Environmental Engineering Division,Korea Institute of Ocean Science and Technology, 787 Haeanro,Ansan 426-744, Republic of Korea*

[b]*Ocean Scisenc & Technology School, Korea Maritime and Ocean University, 727 Taejongro, Yeongdo-Gu, Busan 606-791, Republic of Korea*

Abstract

Edge waves have been reported to pose a threat of inundation to lowland coasts. To illustrate main features of edge waves generated by external forces, we consider two simple examples: landslides moving in the cross-shore direction, and moving atmospheric disturbances parallel to the shoreline. The derivation of a linear shallow water edge wave subject to external force and numerical results are both presented.

Peer- Review under responsibility of organizing committee , IIT Madras , and International Steering Committee of APAC 2015

Keywords: Shallow water linear edge wave; Landslide; Moving atmosphric pressure; Numerical integration; Contour integration.

1. Introduction

Edge waves can be generated by disturbances in coastal areas and are trapped there due to the refraction of long gravity waves over a sloping bottom. Their amplitudes diminish rapidly as we move seaward from the shoreline, and are negligible at a few wavelengths. Thus, their energy is essentially confined within a distance of one wavelength from the coast.

Edge wave can be derived from shallow water equations by Eckard (1951). For a mild sloping beach, the shallow water edge wave is nearly identical to the full linear edge wave obtained by Ursell (1952). These waves propagate along the shoreline in a packet form of time-varying finite extent, but their wave patterns are drastically different

* Corresponding author. Tel.: +82-31-400-6331; fax: +82-31-408-5823.
E-mail address: snseo@kiost.ac

Peer- Review under responsibility of organizing committee , IIT Madras , and International Steering Committee of APAC 2015
doi:10.1016/j.proeng.2015.08.312

from external forces acting on the seawater. We consider two types of edge waves: generated by landslides moving in the cross-shore direction, and moving atmospheric disturbances parallel to the shoreline.

The shallow water edge wave can be constructed in terms of eigenfunctions of the Laguerre differential equation obtained from the Fourier-Laplace transformed equation of the associated shallow water equations. When both unknown and given forcings are expanded in terms of the eigenfunctions, the expansion coefficients in the unknown can be readily determined by orthogonality of the functions. The solution is expressed in integral form resulting from inversion of the Fourier-Laplace transform. Regular integrals with one or both limits being infinite can be evaluated by an appropriate numerical integration method. For singular integral, of which the integrand becomes unbounded at one or more points in the interval, the method of contour integration is applied to convert it to regular integrals, and they can be computed by a numerical integration. The edge wave appears as a dispersive wave because of dispersion relationship obtained in the derivation.

The crest lines of an edge wave generated by a landslide moving in the cross-shore direction show a complicated pattern (Sammarco and Renzi, 2008; Seo and Liu, 2013). In contrast, edge wave patterns generated by moving atmospheric pressure parallel to the shoreline are much simpler, with their crest lines perpendicular to the shoreline (Seo and Liu, 2014). For edge waves generated by a landslide moving in the onshore-to-offshore direction, the solution for surface elevation is expressed by regular integrals. Using numerical integration methods, Seo and Liu (2013) presented accurate results of surface elevation from the beginning of wave generation to a time of interest.

An edge wave generated by a moving pressure disturbance is represented by sum of three singular integrals. The first integral has two singular points which generate a quasi-steady wave behind the pressure center and an additional regular integral of minor contribution. The sum of the other two integrals, with one singular point in each, produces a complementary wave against the quasi-steady wave to generate an edge wave packet of a finite extent behind the pressure center (Seo and Liu, 2014). Once the edge wave packet is generated, the trailing waves occupy roughly the first half of the route of the moving pressure. The edge wave propagates in a packet form when the moving pressure speed is faster than a critical speed; otherwise, only static depression appears according to the inverse barometric rule described by Munk *et al.* (1956).

The edge wave generated by a moving atmospheric pressure receives a constant force on water from the pressure. In contrast, the edge waves generated by a landslide movement on an infinite sloping beach are formed by the landslide forcing with a finite duration. When the landmass moves below a certain depth, its effect on the free surface motion essentially vanishes. After this, consequently, the amplitude of landslide edge wave decreases with time. In the present study, the numerical results of edge waves generated by both landslide and moving atmospheric pressure are presented and their main features are illustrated.

2. Linear shallow water edge waves

Cartesian coordinates are chosen with $\tilde{x}$ pointing out to sea, $\tilde{y}$ coinciding with a straight shoreline and $\tilde{t}$ denoting time. Linear edge waves on a constant sloping beach can be derived from linear shallow water equations with surface elevation $\tilde{\zeta}$ and averaged horizontal velocity $\tilde{\mathbf{u}}$ over small perturbed ground motion $\tilde{b}\left(\tilde{x},\tilde{y},\tilde{t}\right)$ on a uniformly sloping beach $\tilde{h}\left(\tilde{x}\right)=\alpha\tilde{x}$ with bottom slope α.

$$\frac{\partial\left(\tilde{\zeta}-\tilde{b}\right)}{\partial\tilde{t}}+\tilde{\nabla}\cdot\left(\tilde{\mathbf{u}}\tilde{h}\right)=0,\quad \frac{\partial\tilde{\mathbf{u}}}{\partial\tilde{t}}=-\frac{1}{\rho}\tilde{\nabla}\tilde{P}\left(\tilde{x},\tilde{y},\tilde{z},\tilde{t}\right). \tag{1}$$

Based on the shallow water assumption with given atmospheric pressure $\tilde{P}_a$, eliminating the velocity vector from (1) gives

$$g\tilde{\nabla}\cdot\left(\tilde{h}\tilde{\nabla}\tilde{\zeta}\right)-\frac{\partial^2\tilde{\zeta}}{\partial\tilde{t}^2}=-\frac{1}{\rho}\tilde{\nabla}\cdot\left(\tilde{h}\tilde{\nabla}\tilde{P}_a\right)-\frac{\partial^2\tilde{b}}{\partial\tilde{t}^2}. \tag{2}$$

To get the dimensionless equation of (2), physical variables are scaled by typical length a, vertical length ζ_o and reference atmospheric pressure P_o.

$$x=\frac{\tilde{x}}{a},\quad y=\frac{\tilde{y}}{a},\quad \zeta=\frac{\tilde{\zeta}}{\zeta_o},\quad t=\frac{\sqrt{\alpha g}}{\sqrt{a}}\tilde{t},\quad P_a\equiv\frac{\tilde{P}_a}{P_o}=\frac{\tilde{P}_a}{\rho g\zeta_o},\quad b=\frac{\tilde{b}}{\zeta_o}. \tag{3}$$

Then the dimensionless equation of (2) becomes

$$x\frac{\partial^2\zeta}{\partial x^2}+\frac{\partial\zeta}{\partial x}+x\frac{\partial^2\zeta}{\partial y^2}-\frac{\partial^2\zeta}{\partial t^2}=-\left(\frac{\partial P_a}{\partial x}+x\frac{\partial^2 P_a}{\partial x^2}+x\frac{\partial^2 P_a}{\partial y^2}\right)-\frac{\partial^2 b}{\partial t^2}\equiv -q(x,y,t). \tag{4}$$

As for boundary conditions to (4), surface elevation is not only finite at the shoreline but also vanishes away from the shore. Furthermore, since the disturbances are of finite size, no motion is felt at a great distance from the wave generation zone. Before $t=0$, no disturbances are assumed to be in motion.

Because of the imposed boundary conditions, it is convenient to take Fourier and Laplace transforms of (4). We note that the same Fourier pair as in Greenspan (1956) is used to correctly produce the resurgent waves behind a moving pressure center. Using the boundary conditions, the transformed equation to (4) becomes

$$x\frac{\partial^2\overline{\hat{\zeta}}}{\partial x^2}+\frac{\partial\overline{\hat{\zeta}}}{\partial x}-xk^2\overline{\hat{\zeta}}-s^2\overline{\hat{\zeta}}=-\overline{\hat{q}}(x,k,s). \tag{5}$$

To solve non-homogeneous equation (5), we use eigenfunction expansion method, which gives uncoupled linear algebraic equations on the unknown coefficients in the expansion. To this end, employing a change of variables and including negative values of k

$$\xi=2|k|x,\quad \overline{\hat{\zeta}}(x,k,s)=e^{-\xi/2}f(\xi,|k|,s), \tag{6}$$

a non-homogeneous Laguerre differential equation can be obtained as in previous studies (Eckard, 1951; Whitham, 1979). By eigenfunction expansion method , solution of (5) is given by

$$\overline{\hat{\zeta}}(x,k,s)=\sum_{n=0}^{\infty}\frac{e^{-|k|x}L_n(2|k|x)\int_0^{\infty}e^{-\sigma/2}L_n(\sigma)\overline{\hat{q}}(\sigma/2|k|,k,s)\,d\sigma}{(s^2+\omega_n^2)}, \tag{7}$$

where the Laguerre polynomials $L_n(\xi)$ and eigenfrequency ω_n are defined, respectively, by

$$L_n(x)=\sum_{m=0}^{n}\frac{(-1)^m n!x^m}{(n-m)!m!m!};\quad \omega_n^2=|k|(2n+1),\quad n=0,1,2,\cdots. \tag{8}$$

Using inverse Laplace-Fourier transform of (7), the surface displacement can be obtained by taking its real part.

$$\zeta(x,y,t)=\mathrm{Re}\frac{1}{2\pi}\sum_{n=0}^{\infty}\int_{-\infty}^{\infty}e^{-iky}e^{-|k|x}L_n(2|k|x)\,T_n(k,t)\,dk, \tag{9}$$

where

$$Q_n(\nu,k,t)=\int_0^t \hat{q}(\nu,k,\tau)\,\frac{\sin\omega_n(t-\tau)}{\omega_n}d\tau,\quad T_n(k,t)=2|k|\int_0^\infty e^{-|k|\nu}L_n\left(2|k|\nu\right)\,Q_n(\nu,k,t)\,d\nu. \tag{10}$$

All the instances of k in (10) must have absolute sign except the Fourier transform of the input data.

3. Numerical results

In this section we show two examples to demonstrate the present model: edge waves generated by a double Gaussian shape landslide moving in the offshore direction and a hump-shaped atmospheric high pressure moving in the alongshore direction by Munk *et al*. (1956). These external forces produce drastically different wave patterns, propagating along the shoreline in a packet form of time-varying finite extent on constant sloping beach, slope of which is so slight that a shallow water edge wave can be applied.

3.1. Double Gaussian shape landslide without atmospheric forcing

We consider that the landslide has a moving double Gaussian shape in the x direction from an initial position of slide center x_o with speed U . For aspect ratio c, the landslide is given by

$$b(x,y,t)=e^{-(x-x_o-\mathrm{U}t)^2}e^{-(cy)^2}. \tag{11}$$

The forcing function Q_n can be obtained analytically by plugging the Fourier transform of (7) into (10).

$$Q_n(\nu,k,t)=\frac{\sqrt{\pi}}{c}\exp\left(-\frac{k^2}{4c^2}\right)\left\{\begin{array}{l}-2\mathrm{u}(\nu-x_o)e^{-(\nu-x_o)^2}\,\dfrac{\sin\omega_n t}{\omega_n}+e^{-(\nu-x_o-\mathrm{U}t)^2}-e^{-(\nu-x_o)^2}\cos\omega_n t\\ +\mathrm{Im}\left[F(\nu,k,t)\right]\cos\omega_n t-\mathrm{Re}\left[F(\nu,k,t)\right]\sin\omega_n t\end{array}\right\}, \tag{12}$$

where

$$F(\nu,k,t)=\frac{\omega_n\sqrt{\pi}}{2\mathrm{U}}e^{-\omega_n^2/(4\mathrm{U}^2)}e^{i\omega_n(\nu-x_o)/\mathrm{U}}\left[\mathrm{erf}\left(\nu-x_o+i\frac{\omega_n}{2\mathrm{U}}\right)-\mathrm{erf}\left(\nu-x_o+i\frac{\omega_n}{2\mathrm{U}}-\mathrm{U}t\right)\right]. \tag{13}$$

In (12) Q_n is a real-valued function and symmetric in k. Substituting (12) into (9) yields the surface elevation.

$$\zeta(x,y,t)=\frac{1}{\pi}\sum_{n=0}^{\infty}\int_0^\infty\left[e^{-kx}L_n(2kx)\,T_n(k,t)\right]\cos ky\,dk, \tag{14}$$

where T_n is defined as (10) and use is made of symmetry in k. Since double Gaussian landslides allow us to obtain an analytical expression of Q_n, the surface elevation (14) is represented by a double integral in which the upper integral limit is infinity. The improper integral in (14) is computed by routines in "Quadpack" (Piessens *et al*., 1983). These routines are based on globally adaptive interval subdivisions in connection with extrapolation by the epsilon algorithm which accelerates convergence processes in quadrature.

To verify our results, the lateral spreading parameter of Gaussian landslide, c in (11), is set to 2 and the moving speed U is set to 1. Fig. 1 shows the computed surface profiles by a Gaussian landslide at four moments in time frames. In the figure, ζ_n denotes computed elevations added up to the $(n+1)^{\text{th}}$ mode. We have observed that adding together the first ten modes is good enough to accurately represent the surface profile.

For the Gaussian landslide, the symmetric initial condition produces symmetric elevations with respect to $y=0$. At the early phase $t\le 3$, the effect of source-specificness on the solution remains conceivably stronger than any

other propagation phases. The entering landmass has clearly produced a positive wave form on the surface in front of the landmass. A free surface depression is also formed behind the positive wave. In this period of time, generated waves propagate essentially in the seaward direction compared to the alongshore propagation.

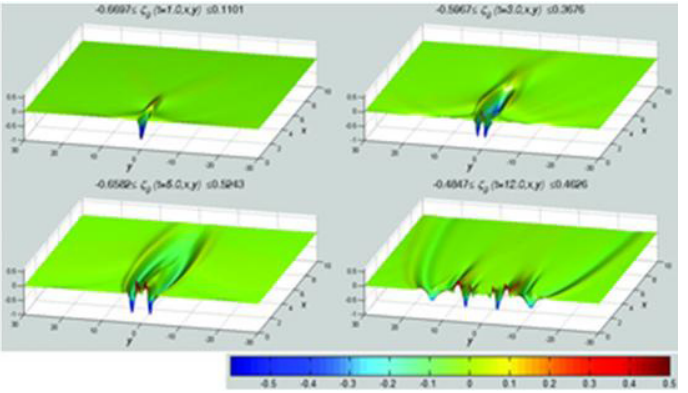

Fig. 1. Snapshots of computed edge waves by a double Gaussian landslide..

As the landmass moves farther down slope, the surface depression produced behind the slide becomes bigger, which in turn develops lateral pressure gradients toward the centerline $(y=0)$. These pressure gradients eventually generate a positive wave form inside the zone of the surface depression, and the positive wave form builds with time. From a series of computed elevations, we observe that the generated waves radiate in all directions, but always within the nearshore region. Therefore we can see a complicated form of edge waves just starting to travel along the shoreline.

As the landmass moves to deeper water, the effects of landslide on the free surface motions diminish. During this period of time, generated waves propagate essentially to the alongshore direction rather than the seaward direction, as shown in Fig. 1. The snapshot at $t=12$ shows that the leading crest of generated wave remains in the computation domain. Because of the faster propagating wave speed in deeper region, the crestline of the leading wave is bent towards to the coast. Hence, offshore waves leave the computational domain first, and nearshore waves follow them in leaving the domain.

It can be clearly seen that the largest amplitude of edge waves occur at the shore. As time goes on, the edge wave amplitude decreases. In the neighborhood of $y=0$, the displacement returns to the undisturbed level so that the generated waves appear within a finite extent. Hence the edge waves, in appearance, propagate in the form of packet waves along the shore.

3.2. Hump-shaped moving atmospheric pressure without landslide

Munk *et al*. (1956) studied a special moving atmospheric high pressure parallel to the shoreline with a constant V, which has a hump-shaped cross-section in the alongshore direction and a singular point at the center $x=x_o$.

$$P_a=\frac{\left(x-x_0\right)}{\left(x-x_0\right)^2+\left(y-Vt\right)^2}. \tag{15}$$

From Fourier transform of (15), the function Q_n in (10) becomes

$$Q_n\left(\nu,k,t\right)=\pi\left|k\right|e^{-\left|k\right|\left(\nu-x_0\right)}\left[\frac{e^{ikVt}}{\left(kV-\omega_n\right)\left(kV+\omega_n\right)}-\frac{e^{i\omega_n t}}{2\omega_n\left(kV-\omega_n\right)}+\frac{e^{-i\omega_n t}}{2\omega_n\left(kV+\omega_n\right)}\right]. \tag{16}$$

In contrast to the landslide as in (12), this function Q_n has three singular integrals in the complex k plane, and more work is needed to evaluate the integrals. And function T_n becomes

$$T_n(k,t)=\pi|k|e^{|k|x_0}\left[\frac{e^{ikVt}}{\left(k^2V^2-\omega_n^2\right)}-\frac{e^{i\omega_n t}}{2\omega_n\left(kV-\omega_n\right)}+\frac{e^{-i\omega_n t}}{2\omega_n\left(kV+\omega_n\right)}\right]\int_0^\infty e^{-2|k|v}L_n\left(2|k|v\right)2|k|dv. \tag{17}$$

Due to the special form of (15), surface elevation results in only one mode which gives a significant simplification in analysis. Using $k^2=|k|^2$, $\omega_0^2=|k|$ and fundamental wave number $k_0=1/V^2$, we obtain non-dimensional equation (18) obtained by Greenspan (1956).

$$\zeta(x,y,t)=\frac{1}{2}\int_{-\infty}^{\infty}e^{-|k|(x-x_0)}\left[\frac{k_0e^{-ik(y-Vt)}}{|k|-k_0}+\frac{|k|e^{-i(k\,y-\omega_0 t)}}{2\left(|k|-k\sqrt{|k|/k_0}\right)}+\frac{|k|e^{-i(k\,y+\omega_0 t)}}{2\left(|k|+k\sqrt{|k|/k_0}\right)}\right]dk. \tag{18}$$

Surface elevations in (18) is represented by a sum of three singular integrals. When the moving speed is equal to wave speed, the integrand blows up but the integrals are bounded, as will be shown shortly. To evaluate these singular integrals, we will use the method of contour integration in the complex plane. One crucial point in performing the contour integration essentially resides in the representation of $|k|$ on the complex plane.

Evaluation of the first integral depends on relative poistion to the pressure center Vt. The contribution from two poles produces the quasi-steady wave behind the pressure center, valid only for $0\le y<Vt$, and plays a dominant role. And an additional regular integral makes a smooth transition of the surface elevation in the neighborhood of the pressure center, where the sea surface is also directly deformed by the pressure distribution according to the inverse barometer rule.

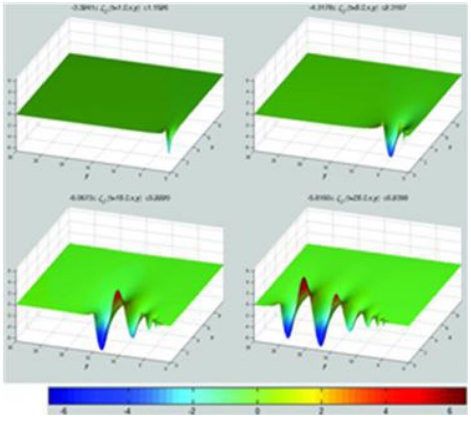

Fig. 2. . Snapshots of computed edge waves by hump-shaped pressure distribution with parameters $x_0=-0.1$ and $V=1$ ..

For the second integral in (18), there is no contribution from the pole in both contours. In evaluating contour integrals along the branch lines, a branch cut for square root is needed which is taken on the non-negative real axis. Because the exponential term on the resultant equation from the contour integraton, this regular integral is easily computed by a numerical integration method and makes a very small contribution to the final result. In a similar way to the second integral, a regular integral can be obtained. Since the exponential term in the integrand does not show monotonic decay with integration dummy variable, some difficulties in evaluation are readily anticipated, which essentially depend on the relative magnitude between y and t in the exponential term. However, the third integral is eventually bounded by self-cancellation due to high oscillations of the integrand as the dummy variable increases. Consequently, care must be taken to address the difficulty, as shown in Seo and Liu (2014).

Due to the definition of non-dimensional variables in (3) and the derived surface elevation in (18), the elevation is affected by both the bottom slope and atmospheric properties such as shape, disturbance size, pressure anomaly, moving speed, and center position. We illustrate edge waves generated by a moving high atmospheric pressure but an edge wave generated by a low pressure system has only sign difference compared to that by a high pressure system.

Fig. 2 shows the computed surface elevations at different times of an edge wave generated by a hump-shaped pressure distribution with parameters $x_0 = -0.1$ and $V = 1$, in which the pressure center is located on land along $(-0.1, t)$. Early on, at $t = 1$, we can clearly see that the static effect of the pressure distribution on the sea surface is dominant. As time progresses, an edge wave packet is formed, which results from the interaction between the quasi-steady wave and the complementary wave. The extent of the edge wave packet increases with time, and trailing waves have decreasing amplitude away from the moving pressure center. It is also clearly shown that the largest amplitude appears at the shore, and a quick decrease in amplitude in the offshore direction confines the waves to the vicinity of the shore. At the top of each panel, the computed extreme values are presented.

In Fig. 3, the surface elevation at the shoreline is plotted for different moving speeds at $t = 30$. In order to show the difference clearly between the edge wave from all components (black line), the quasi-steady wave (red dotted line) and the contribution from branch cut lines of the first integral (blue dashed line), the quasi-steady wave is plotted over the same range even though it is valid only behind the pressure center. It can be concluded from the result that in the rear of the wave packet, the quasi-steady wave should not be used as an approximation of the edge wave. And the complementary wave affects both the reducing amplitude and the changing phase.

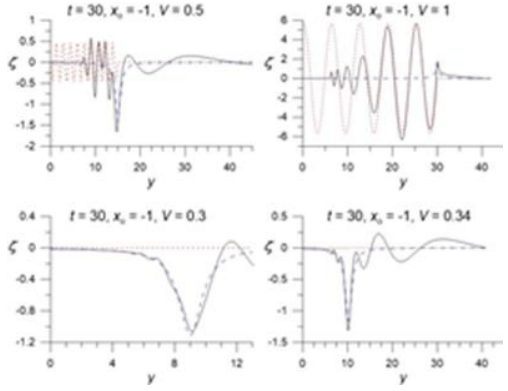

Fig. 3. Comparison of surface elevations at the shoreline by a hump-shaped moving pressure with $x_0 = -1$ and different speeds at $t = 30$.

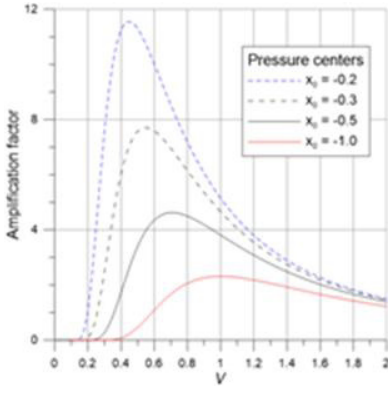

Fig. 4. Amplitudes of quasi-steady wave at the shoreline for a hump-shaped moving pressure with different speeds and centers.

For $V = 0.3$, evidently the static depression (blue dashed line) is produced by the regular integrals in the first integral, because the elevation of the quasi-steady wave is drawn in a straight line with nearly zero height. If a moving speed is slower than a critical speed, static depression is dominant with small wave packets developed both in front of and behind the pressure center which moves together with the atmospheric pressure. The static depression is virtually the same as the surface drop in this figure resolution by the given pressure distribution, according to the inverse barometric rule. The critical speed may be defined by a speed to produce the amplitude of the fundamental mode in the quasi-steady wave less than 0.01 in the present scale.

As moving speed exceeds the critical speed, a wavy form on the free surface starts to be built up. For $V = 1$, the quasi-steady wave has an amplitude of $2\pi k_0 \exp\left[-k_0\left(x - x_0\right)\right]$, which shows a good approximation of the edge wave in an interval from the pressure center to a point behind it. According to Greenspan (1956), this point is given as $0.5Vt$ and from this point to the origin $\left(0 < y < 0.5Vt\right)$ surface elevation returns to the still water level. However, we can see considerable deviation from Greenspan's approximation. The rear part of a packet which is heavily affected by the complementary wave has a significantly different shape from that of the front waves.

In Fig. 4, the amplification factors of the quasi-steady wave at the shoreline are plotted for a hump-shaped moving pressure against varying speeds. As pointed out before, the amplitude of the quasi-steady wave depends on both the moving speed and pressure center location on land.

We have conducted several numerical experiments in examining the surface elevation profiles for slow-moving systems. Because of the factor $k_0 = 1/V^2$ in the quasi-steady wave, slow-moving pressures, which roughly mean a larger system, create bigger waves. When the pressure center is at an inland point farther away from the shoreline, the amplification factor is reduced appreciably. Moreover, when $x_0 = -1$, it can be anticipated that only static depression in the first integral occurs for $V \le 0.3$, in which the amplification factor amounts to 0.001. For a given position x_0, the maximum amplitude for a hump-shaped pressure occurs at $V = \sqrt{-x_0}$, which can be obtained by finding the maximum of the quasi-steady wave amplitude at the shoreline with respect to k_0. Thus, a distant moving disturbance from the shoreline produces the maximum amplitude at a higher speed.

4. Conclusions

Since edge waves have the largest amplitude at the shore and quick decay in amplitude away from the shoreline, they can pose the threat of inundation to lowland coastal areas. A shallow water edge wave consists of an infinite number of modes, being essentially confined within a distance from the shore, and propagates along the shoreline in a packet form of time-varying finite extent due to the celerity difference of component waves in the packet.

The crest lines of an edge wave generated by a landslide moving in the cross-shore direction on an infinite sloping beach show a complicated pattern. These edge waves are formed by the landslide forcing which affects free surface motion only within a finite duration. When the landmass moves below a certain depth, the effect of it on the free surface motion essentially vanishes. After that, consequently, the amplitude of landslide edge wave decreases with time. Through numerical experiments, the largest amplitude is found to occur at the shore and a packet of waves propagates along the shoreline. The leading edge wave does not have the highest amplitude and the largest one appears in the middle of the packet. With increasing time, wave crests are created in the course of propagation as in the case of constant depth.

In contrast, edge wave patterns generated by moving atmospheric pressure parallel to the shoreline are much simpler, with their crest lines perpendicular to the shoreline. These edge waves are generated by a constant forcing on water from a moving atmospheric pressure. In numerical experiments, it has clearly been shown that the edge wave propagates in a packet form when the moving pressure speed is faster than a critical speed. For many cases, the quasi-steady wave can give a reasonable approximation of the waves only in the first half of a wave packet. Because of this distinctive feature, the amplitude of waves in the first half of a wave packet is almost constant after an edge wave packet has been fully developed.

Acknowledgements

This work was supported in part by Korea government research project under grant PM58331, and by KIOST project, PE99325.

References

Eckart, C., 1951. Surface waves in water of variable depth. Scripps Inst. Ocean. Wave Report 100, Univ. of California, La Jolla.

Greenspan, H.P., 1956. The generation of edge waves by moving pressure distributions. *J. Fluid Mech.*, 1, 574-590.

Munk, W., Snodgrass, F., Carrier, G., 1956. *Science* 123, 127-132.

Piessens, R., De Doncker, E., Uberhuber, C., Kahaner, D., 1983. Quadpack – A subroutine package automatic integration. Springer-Verlag, Berlin.

Sammarco, P., Renzi, E., 2008. Landslide tsunami propagating along a plane beach. *J. Fluid Mech.*, 598, 107-119.

Seo, S.N., Liu, P. L.-F., 2013. Edge waves generated by the landslide on a sloping beach. *Coastal Eng.* 73, 133-150.

Seo, S.N., Liu, P. L.-F., 2014. Edge waves generated by atmospheric pressure disturbances moving along a shoreline on a sloping beach. *Coastal Eng.* 85, 43-59.

Ursell, F., 1952. Edge waves on a sloping beach. *Proc. R. Soc. Lond. Ser. A*, 214, 79–97.

Whitham, G.B., 1979. Lectures on wave propagation. Springer-Verlag, New York.